











OPEN

DATA DESCRIPTOR

QUIN 2.0 - new release of the QUaternary fault strain INdicators database from the Southern Apennines of Italy

Giusy Lavecchia ^{1,2,16}, Simone Bello ^{1,2,3,16} ✉, Carlo Andrenacci ^{1,2}, Daniele Cirillo ^{1,2}, Federico Pietrolungo^{1,2}, Donato Talone^{1,2}, Federica Ferrarini ^{1,2}, Rita de Nardis^{1,2}, Paolo Galli ^{4,5}, Joanna Faure Walker ⁶, Claudia Sgambato⁷, Marco Menichetti ^{2,8}, Carmelo Monaco^{2,9,10}, Salvatore Gambino^{2,9}, Giorgio De Guidi^{2,9}, Giovanni Barreca^{2,9}, Francesco Carnemolla^{2,9}, Fabio Brighenti^{2,9}, Salvatore Giuffrida^{2,9}, Claudia Pirrotta⁹, Filippo Carboni^{2,11,12}, Luigi Ferranti^{2,13}, Luisa Valoroso¹⁴, Giovanni Toscani^{2,15}, Massimiliano R. Barchi^{2,12}, Gerald Roberts⁷ & Francesco Brozzetti^{1,2}

QUIN database integrates and organizes structural-geological information from published and unpublished sources to constrain deformation in seismotectonic studies. The initial release, QUIN1.0, comprised 3,339 Fault Striation Pairs, mapped on 445 sites exposed along the Quaternary faults of central Italy. The present Data Descriptor introduces the QUIN 2.0 release, which includes 4,297 Fault Striation Pairs on 738 Structural Sites from southern Italy. The newly investigated faults span ~500 km along the Apennines chain, with strikes transitioning from ~SE to ~SW and comprehensively details Fault Striation Pairs' location, attitude, kinematics, and deformation axes. Additionally, it offers a shapefile of the fault traces hosting the data. The QUIN 2.0 release offers a significant geographic extension to the QUIN 1.0, with comprehensive description of local geometric-kinematic complexities of the regional pattern. The QUIN data may be especially relevant for constraining intra-Apennine potential seismogenic deformation patterns, where earthquake data only offer scattered or incomplete information. QUIN's data will support studies aimed at enhancing geological understanding, hazard assessment and comprehension of fault rupture propagation and barriers.

Background & Summary

Open shared databases in seismic hazard research provide a landmark platform for scientists, researchers and policymakers to access and analyse vast geological and seismological data, enabling a deeper understanding of earthquake hazards and improving our ability to assess and mitigate seismic risks.

¹DiSPuTer, Università degli Studi "G. d'Annunzio" Chieti-Pescara, Chieti, Italy. ²CRUST - Centro interUniversitario per l'analisi Sismotettonica Tridimensionale, Chieti, Italy. ³CNR, Istituto di Geologia Ambientale e Geoingegneria, Monterotondo 00016 Rome, Italy. ⁴Dipartimento della Protezione Civile, 00193, Rome, Italy. ⁵Istituto di Geologia Ambientale e Geoingegneria (IGAG) del Consiglio Nazionale delle Ricerche (CNR), Monterotondo 00016, Rome, Italy. ⁶Institute for Risk and Disaster Reduction, University College London, London, UK. ⁷Department of Earth and Planetary Sciences, Birkbeck, University of London, London, UK. ⁸Università degli Studi di Urbino Carlo Bo, Urbino, Italy. ⁹Dipartimento di Scienze Biologiche Geologiche e Ambientali, Università di Catania, 95129, Catania, Italy. ¹⁰Istituto Nazionale di Geofisica e Vulcanologia, Osservatorio Etneo-Sezione di Catania, Catania, Italy. ¹¹Institute of Earth and Environmental Sciences (Geology), Albert-Ludwigs-University Freiburg, Freiburg, Germany. ¹²Dipartimento Fisica e Geologia, Università Degli Studi di Perugia, Perugia, Italy. ¹³DiSTAR, Università degli Studi di Napoli Federico II, Naples, Italy. ¹⁴Istituto Nazionale di Geofisica e Vulcanologia, Rome, Italy. ¹⁵Dipartimento di Scienze della Terra e dell'Ambiente, Università di Pavia, Pavia, Italy. ¹⁶These authors contributed equally: Giusy Lavecchia, Simone Bello. ✉e-mail: simone.bello@unich.it

In a recent Data Descriptor¹, QUIN (QUaternary fault strain INDicators) was introduced as a comprehensive geological database designed to integrate and organize geological information to analyse Quaternary deformation and strain, primarily for seismotectonic studies and geodynamic modeling. The initial release¹ focused on the Northern and Central Apennines extensional belt and included structural field data on fault geometry and kinematics: specifically, 3,339 Fault Striation Pairs (hereinafter “FSPs”) mapped at 445 Structural Sites (hereinafter “SSs”) and derived strain indicators were included in the database. Given that the regional stress field in Italy has remained relatively unchanged over the last 3 million years^{2–4}, it is feasible to extend the observation of structural data relevant to seismogenic purposes at least to the entire Quaternary period, encompassing the last 2.58 million years⁵. Covering the extension back this far opens up a wealth of data that can significantly improve our understanding of present deformation patterns which often appear incomplete when relying just on earthquake data.

Open-access databases on present-day stress patterns are widely available in the literature (e.g.^{6–12}). However, they primarily rely on indicators such as focal mechanisms, borehole breakouts, and overcoring data. Less information is available on geological fault data, which might provide insights into stress variations at the local and regional fault scale (e.g.^{13–21}). In this regard, Italy stands out as an exception. Indeed, due to the excellent exposure conditions of the intra-Apennine normal faults and their accessibility, some fault/slip databases are available in the literature (e.g.^{22–26}), but they do not refer to southern Italy and do not provide detailed strain pattern data as those given in the QUIN database.

The methodology employed in QUIN and the criteria used to compile the database were fully described by Lavecchia *et al.*¹, together with its main features and applications. Lavecchia *et al.*¹ also included examples illustrating how the database can be used to investigate the entral Apennines region’ seismic potential and deformation patterns. We here present the QUIN 2.0 database which extends the coverage to the Quaternary extensional faults in the Southern Apennines of Italy and Sicily, along a length of ~500 km (Figs. 1, 2). QUIN 2.0 incorporates a wide collection of FSP records, including both unpublished (2006) and literature data (2291), distributed along 738 SS. For each FSP, the database provides information on the major Quaternary fault hosting the SS (Host Fault, hereinafter “HF”), geometric and kinematic parameters, and a quality assessment of the data. The additional FSP records of the QUIN 2.0 significantly enlarge the area considered by QUIN 1.0 (Fig. 1), providing a comprehensive view of the potential seismogenic structures of Central and Southern Italy.

The Southern Apennines area is characterized by an interconnected pattern of normal-to-oblique faults that generated some of the most destructive earthquakes in Italy²⁷, such as the Campania-Lucania 1980 earthquake (M_w 6.9)²⁸, the Messina Strait 1908 earthquake (M_w 7.1)^{29–31}, the Basilicata 1857 earthquake (M_w 7.1)^{32–35}, the Southern Calabria 1783 seismic sequence (M_w 7.1)^{31,36,37} and the March-June 1638 Central Calabria earthquakes (M_w 7.1)^{38,39}. Despite this, in contrast to the Central and Northern Apennines^{21,40–47}, since 1981 the area has undergone only minor-to-moderate seismicity (M_{wmax} 5.7⁴⁸) with a consequent lack of extensive information on the active (instantaneous) and seismogenic stress field.

The long-term structural data provided by QUIN 2.0 advances the understanding of the Quaternary deformation patterns in the Southern Apennines of Italy and Sicily, providing valuable insights for seismotectonic studies and related research fields. The database can be integrated with geodetic⁴⁹ and seismological data to carry out formal stress inversions at the regional scale. This is useful for investigating local-scale effects that control active deformation, seismogenic faulting, and seismic hazard in a region where high seismogenic potential is suggested by both historical seismicity and Quaternary faults, even if only moderate seismicity was recorded in instrumental times. Furthermore, the database can be exploited for further elaborations on structural analysis, high-detail fault segmentation and distribution (e.g.^{50–53}), geodynamic reconstructions and seismic hazard as well as for geothermal and petroleum exploration.

By freely sharing and collaborating on multidisciplinary data and fully integrating structural and seismological data, the scientific community can foster innovation, accelerate seismotectonic research progress, and facilitate evidence-based decision-making, ultimately leading to more effective earthquake preparedness and resilience strategies.

Methods

QUIN 2.0 Database: structure and building process. The development of the QUIN 1.0 database¹ involved a systematic approach, integrating existing data from the literature with newly acquired information. The database was aimed to create a comprehensive and detailed repository of Quaternary fault/slip data for the Northern-Central Italy intra-Apennine extensional belt. In this second release, focused on the extensional belt of southern peninsular Italy and north-eastern Sicily, we followed the same approach and method introduced for QUIN 1.0, which we briefly recall below. A complete description of the QUIN database’s structure, building process and usage, can be found in the first release¹.

The QUIN database-building process consists of several key steps needed for the database’s comprehensive-ness. First, we reviewed literature sources to gather relevant fault-related data. Second, we incorporated new and unpublished data from the present paper’s authors. Third, we carried out targeted campaigns to collect missing information and bridge data gaps in the database. These campaigns involved field surveys, geological mapping, and fault plane analysis. The acquired data were integrated into the database, ensuring a complete coverage of FSPs and SSs. The latter, in the QUIN database, are grouped into four distinct categories based on their proximity and characteristics concerning the HFs: (1) SS located on or near the main HF trace within its damage zone, (2) SS representing syn-kinematic faults outside the HF damage zone, (3) SS consisting of faults observed along structures antithetic to the HF, and (4) SS comprising scattered Quaternary fault planes, not directly related to any major HF. This categorization system facilitates efficient organization and retrieval of data. A quality control process was implemented to ensure data accuracy and reliability. Data validation and verification procedures

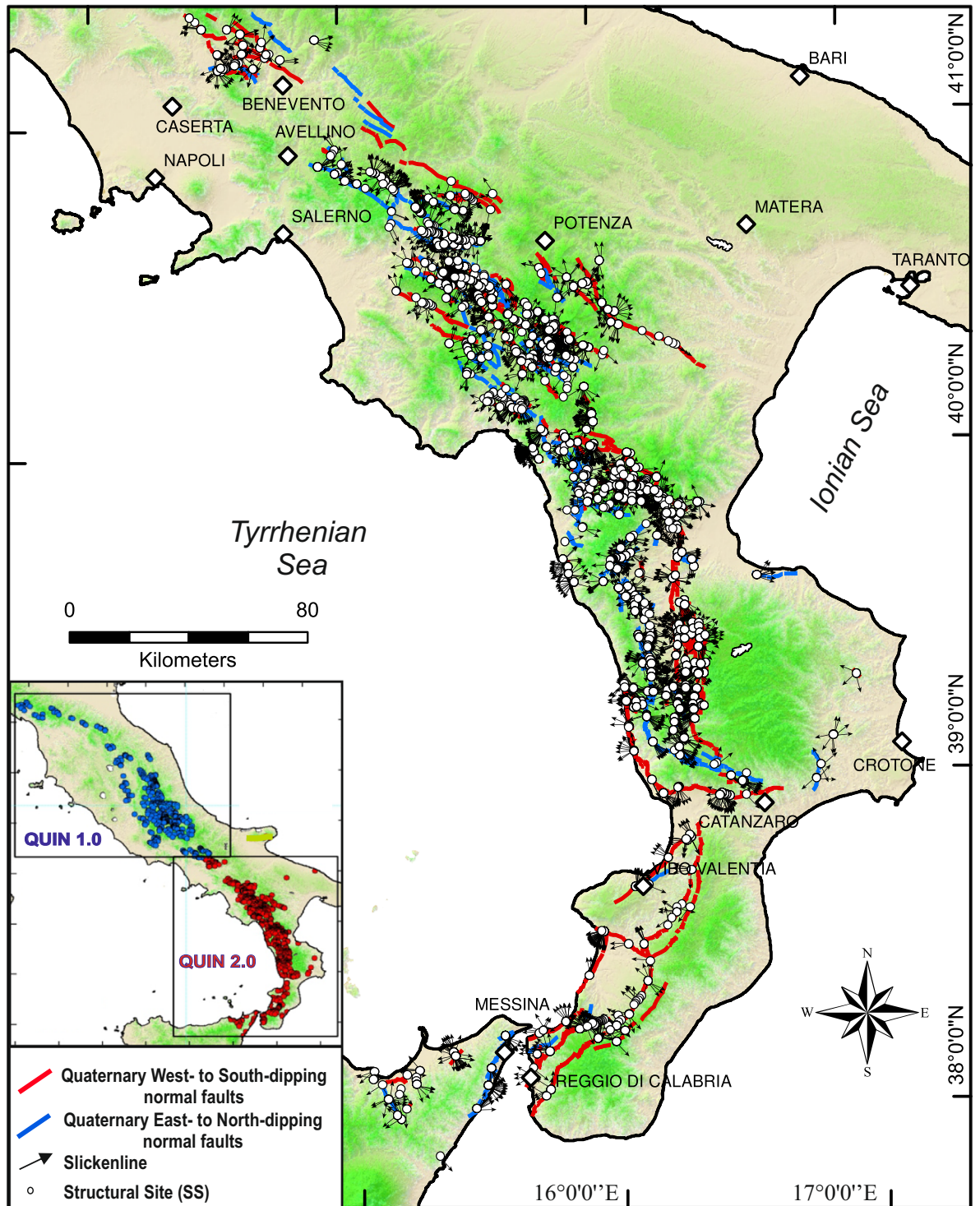


Fig. 1 Map view of the QUIN 2.0 database projected on a shaded relief map of the Southern Apennines of Italy and northeastern Sicily along the trace of the faults (red and blue lines) hosting the QUIN's data (*i.e.*, HF). White circles represent the location of the 738 SS while arrows indicate the slip direction of each of the 4297 FSP. The inset shows the data coverage of the QUIN 1.0¹ (Northern and Central Apennines) and the QUIN 2.0 releases (Southern Apennines and northeastern Sicily).

were performed to identify and rectify possible inconsistencies or errors. Detailed information may be found in Lavecchia *et al.*¹.

Starting from the FSPs data, we perform kinematic analysis and deformation axes calculation. After calculating the rake values (Aki and Richards⁵⁴ convention), we classify the FSPs in kinematic classes corresponding to pitch ranges of 0–30° for strike-slip faults, 30–60° for oblique faults, and 60–90° for dip-slip faults (see Data

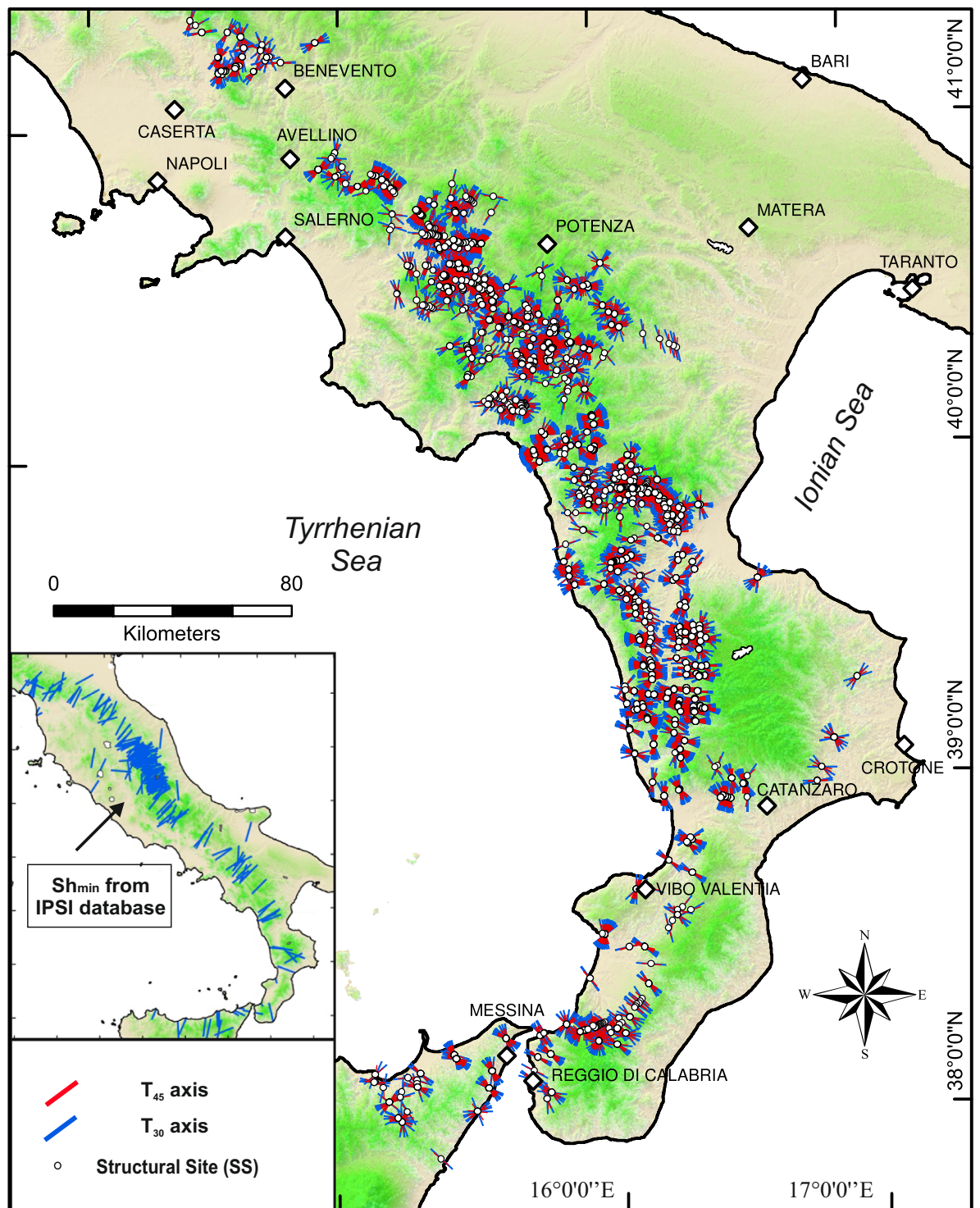


Fig. 2 T_{30} - and T_{45} -axis computed in this database from the input fault/striation pairs data (see next section), on a shaded relief map of the Southern Apennines of Italy and northeastern Sicily. The inset shows the Sh_{min} orientation from the IPSI focal mechanism database^{7,9} for comparison with the QUIN database (see “Technical validation” section).

Record section). Additionally, the attitudes of the principal deformation axes are determined based on two scenarios: a compressional axis at 30° or 45° in the slip plane. The first scenario rests on Anderson’s theory, which suggests an angle of ~30° between the rupture plane and the maximum principal stress (σ_1) in the upper crust. The second scenario considers conventional P-T deformation axes at 45°, as obtained from focal mechanisms and classically used for an initial depiction of SH_{min} horizontal trajectories. The theory beneath the previous

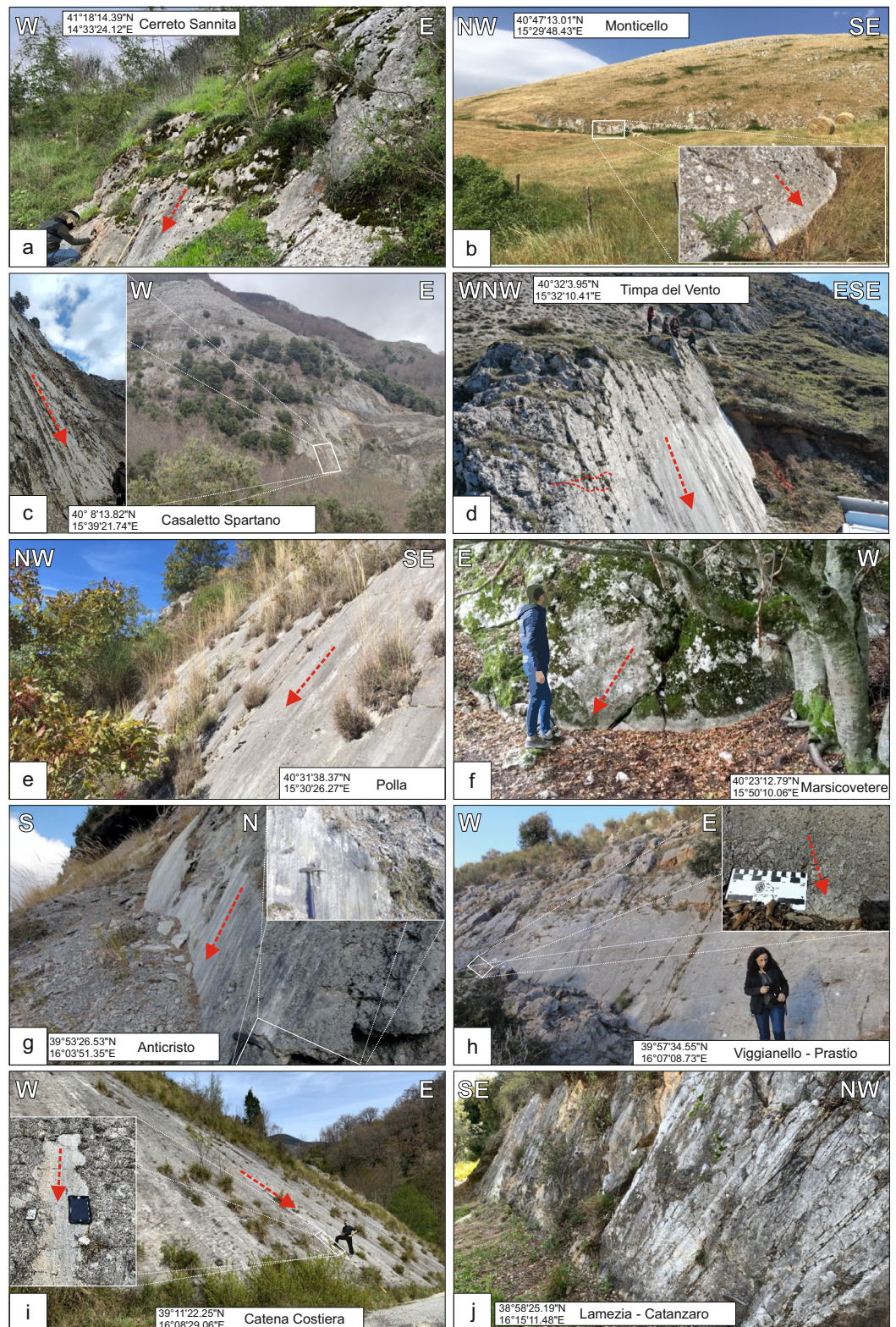


Fig. 3 Photographic documentation of some of the fault planes cropping out along the Southern Apennines extensional belt of Italy included in the QUIN 2.0 database. Each photograph has coordinates reported and the slickenlines (red arrows) drawn.

choices is discussed in Lavecchia *et al.*¹. The above calculations and graphic representations are performed using the *F-SPA tool* specifically developed in MATLAB by Andrenacci *et al.*⁵⁵ for use in QUIN.

Thematic group A: FSP identification and SS location											
Ord_No	SS	FSP	Lon	Lat	Reg	Loc	SS_Pos	Seism	Fault	F_Acronym	F_DipDir
293	MONPAR2	MONPAR2h	15.45300	40.74225	Basilicata	Muro_Lucano	1		Monte_Paratiello	MONPAR	NNE
294	SENER1	SENER1b	15.20040	40.74207	Campania	Senerchia	1	Irpinia_1980_Eq	Senerchia	SENER	E
295	IF8	IF8a	15.31151	40.74028	Campania	Colliano	1	Irpinia_1980_Eq	Irpinia	IF	NE
296	MONTC7	MONTC7a	15.59407	40.73859	Basilicata	Bella	1	Irpinia_1980_Eq	Monticello	MONTC	SSW
297	MONPAR3	MONPAR3a	15.48540	40.73841	Basilicata	Muro_Lucano	1		Monte_Paratiello	MONPAR	NNE
298	MONPAR3	MONPAR3b	15.48540	40.73841	Basilicata	Muro_Lucano	1		Monte_Paratiello	MONPAR	NNE
Thematic group B: FSP geometry, quality ranking and references											
Strike	Dip_dir	Dip	Trend	Plunge	Rake	Kin	Q_loc	Q_res	Ref		
281.0	11.0	64.0	327.7	56.2	-67.6	LN	A	A	Bel21		
356.0	86.0	57.0	112.1	54.1	-104.9	PN	A	A	Sga20		
315.0	45.0	60.0	45.0	60.0	-90.0	PN	A	A	PP		
141.0	231.0	56.0	190.5	48.4	-64.5	LN	A	A	Bel21		
250.0	340.0	85.0	68.2	19.5	-160.4	RS	B	A	PP		
254.0	344.0	74.0	59.7	40.7	-137.3	RS-N	B	A	PP		
Thematic group C: FSP deformation axes											
P45_Trend	P45_Plunge	B45_Trend	B45_Plunge	T45_Trend	T45_Plunge	P30_Trend	P30_Plunge	B30_Trend	B30_Plunge	T30_Trend	T30_Plunge
228.7	63.8	90.7	20.1	354.7	16.1	264.4	69.8	90.7	20.1	360.0	2.0
226.5	73.4	4.3	12.5	96.7	10.8	166.8	76.9	4.3	12.5	273.4	3.8
225.0	75.0	135.0	0.0	45.0	15.0	11.3	90.0	135.0	0.0	45.0	0.0
104.0	67.6	306.0	20.9	213.1	7.7	144.4	68.0	306.0	20.9	38.5	6.3
115.7	17.3	263.7	69.8	22.6	10.1	100.1	19.5	263.7	69.8	8.2	5.3
120.5	41.0	270.6	44.9	16.6	15.4	100.6	44.6	270.6	44.9	5.6	5.0

Table 1. Quin 2.0 thematic groups with examples of records.

Host faults and their tectonic context. Following Lavecchia *et al.*⁵⁶, an updated and detailed review of the HF traces was performed in the present Data Descriptor and a new fault traces map was carried out on a GIS platform (Fig. 1). The database is stored in ZENODO⁵⁷ in shapefile format (.shp) and contains 245 HF records. The related attribute table provides information on the individual HF name and dip direction, as well as on the name and the age of activity (i.e., fault onset) of the fault system containing the HFs. Furthermore, in the attribute table we report information on the possible involvement of the fault in historical/instrumental earthquakes. The QUIN 2.0 HF database covers ~500 km of the Campania, Lucania, and Calabria extensional belt in Southern Italy, encompassing the Peloritani mountains in northeastern Sicily^{58–61}. The fault traces were extracted from the literature and were integrated/updated with data from unpublished maps related to the newly acquired FSPs (i.e., collected in the new field campaigns). In particular, we consulted the online version of the Structural and Neotectonic Models of Italy (scale 1:500,000; <https://www.socgeol.it/438/structural-model-of-italy-scale-1-500-000.html>), the ITHACA catalog (<https://sgi.isprambiente.it/ithaca/viewer/>) and the sheets of the Geological Map of Italy at 1:100,000 (<http://sgi.isprambiente.it/geologia100k/>) and 1:50,000 (<https://www.isprambiente.gov.it/Media/carg/>) scales. Other detailed traces of Late Pleistocene-Holocene faults, accessible on online maps and repositories, together with all the published papers also used to compile the QUIN fault/slip database, were also considered^{17,19,26,28,30,35,36,61–97}. We opted not to utilize the DISS database (<https://diss.ingv.it/>) for QUIN host faults, as it serves different applications and lacks the requisite details for our specific purposes. We derived the age of the fault-systems' activity from the geological literature^{3,28,35,38,62,63,65,98–109} and from the evidence of earthquake activity in historical and instrumental times^{27,110}.

The HFs included in the QUIN 2.0 database⁵⁷ affect different lithologies across the extensional belt. In Campania and Lucania regions, the faults displace platform-to-basinal Meso-Cenozoic limestones, Cenozoic siliciclastic turbidites and Pliocene-Quaternary clastic infill of intra-Apennine extensional basins^{66,98,108,111,112}. Conversely, in Calabria, the normal faults either mark the contact between the Pliocene-Quaternary infill of extensional basins and the crystalline basement or displace the crystalline basement^{80,113,114}. Representative examples of well-exposed fault planes from different locations of the Southern Apennines are reported in Fig. 3.

The Southern Apennines of Italy have undergone extensive deformation over time, resulting in a presently complex geometric and kinematic setting. The Quaternary extensional belt dissects a pre-existing Mio-Pliocene fold-and-thrust belt (e.g.^{58,115,116}). The Miocene-Pliocene compressional phase was driven by the convergence of the Eurasia and Nubia plates, involving the opening of the Tyrrhenian Sea and the deformation of the western Adria Plate^{59,112,117}. As a result, both the compressional structures and the younger normal faults exhibit an

arcuate orientation across the region, ranging from NW-SE in Campania-Lucania to N-S in northern Calabria and NE-SW in southern Calabria and the Peloritani Mountains of Sicily.

Figure 1 shows the alignment of the extensional HF in Southern Italy. Crustal stretching has been suggested to have formed both low-angle (LANFs) and high-angle (HANFs) normal faults⁶⁶. According to some authors^{118–120}, the LANFs in the internal (*i.e.*, western) side of the extensional belt are associated with an early extensional stage preceding the formation of high-angle normal faults bounding the Quaternary basins. Other authors highlight the contemporaneous activity of east-dipping and antithetic west-dipping faults bounding the major intra-mountains Quaternary basins^{66,98,107,121}. The timing of the onset of extensional tectonics also is debated. Some authors propose a regional strike-slip phase during the early stages of intramountain basin development^{122–124}, while others argue for dominant extensional tectonics during the same period^{66,98}. The age of activity for high-angle extensional tectonics ranges from the Late Pliocene to Early Pleistocene and may become progressively younger toward the east, at a regional scale³.

Data Records

The new FSPs data in QUIN 2.0 are 2,006, while data from the literature are 2,291, for a total of 4,297 FSPs data, grouped in 738 SS distributed quite homogeneously along the intra-Apennines Quaternary faults of the Southern Apennines. Both new and previous FSPs are quality selected (see the “Technical Validation” section) and elaborated to obtain kinematic and deformation axes information. QUIN 2.0 database is stored and available in the Zenodo repository¹²⁵ both in shapefile (.shp) and text (.txt) format.

To make the QUIN 2.0 data tables fully mergeable with QUIN 1.0 and even to promote the future use of integrated databases, we maintained the same structure (Table 1). Therefore, the records are organized into 34 fields, each referring to a single FSP. The 34 fields are organized into three thematic groups (A, B, C) defined as follows: A) FSP identification and SS location (fields 1 to 12); B) FSP geometry, quality ranking and references (fields 13 to 22); C) FSP deformation axes (fields 23 to 34).

In addition to the QUIN 2.0 release, we also provide a new release of the HF database with this Data Descriptor. The database is stored in Zenodo⁵⁷ as a shapefile (.shp) and contains 245 linear records (polylines) of the faults hosting the FSPs or neighboring them, traced on a GIS platform. We kept the same structure as the QUIN 1.0 HF table of contents to make the records mergeable. A map view representation of the QUIN 2.0 HF is offered in Fig. 1.

QUIN 2.0 database records description. In the following, we provide a brief description of each field of the QUIN 2.0 database and of the HF database (in brackets the short names reported in the QUIN’s table):

- 1) Ordinal Number (Ord_No): uniquely identifies each FSP.
- 2) Survey Site (SS): contains one or more FSPs; “OF” (Off fault) is reported for those SSs not associated to a certain fault.
- 3) FSP identification Code (FSP): expressed as the acronym of the fault containing the SS, plus a cardinal number which refers to the Survey Site (SS) and a lowercase letter to identify the individual FSP; “OF” (Off fault) is reported for those FSPs not associated to a certain fault.
- 4) Longitude (Lon) of the FSP in decimal degrees (WGS84).
- 5) Latitude (Lat) of the FSP in decimal degrees (WGS84).
- 6) Region (Reg): administrative region of the data location.
- 7) Locality (Loc): municipality of the data location.
- 8) Position (SS_Pos): position and prevailing dip-direction of the SS with respect to the Host Fault (1 = SS located on or near the main fault trace within the damage zone; 2 = SS representing syn-kinematic faults outside the damage zone; 3 = SS consisting of faults observed along antithetic structures; 4 = SS comprising scattered Quaternary fault planes).
- 9) Coseismic Displacement (Seism): it reports when the SS is located on a fault plane displaced during an instrumentally recorded seismic event (earthquake name and year reported); “NaN” = no information.
- 10) Host Fault (Fault): name of the Quaternary fault hosting the SS; “OF” (Off fault) is reported if the FSP is not associated to a fault.
- 11) Host Fault Acronym (F_Acronym): acronym of the fault hosting the SS; “OF” (Off fault) is reported if the FSP is not associated to a fault.
- 12) Host Fault Dip-Direction (F_DipDir): approximate direction of the Host Fault (expressed with respect to the North); “OF” (Off fault) is reported if the FSP is not associated to a fault.
- 13) Strike (Strike; in degrees): azimuth angle of a FSP plane with respect to the North.
- 14) Dip direction (Dip_dir; in degrees): direction of the fault plane dip with respect to the North, expressed with the right-hand rule strike direction.
- 15) Dip angle (Dip; in degrees): angle of dip of the fault plane measured.
- 16) Trend (Trend; in degrees): direction of the slip vector.
- 17) Plunge (Plunge; in degrees): dip of the slip vector.
- 18) Rake: (Rake) calculated using the Aki-Richard’s annotation⁵⁴.
- 19) Rake-based kinematics (Kin): fault regimes classification (PN = Pure dip-slip Normal fault; NF = Normal fault; NS = Normal Strike; SN = Strike Normal; SSL = Strike-Slip Left; SSR = Strike-Slip Right; PSS = Pure Strike-Slip). Further information on rake ranges can be found in Andrenacci *et al.*⁵⁵.
- 20) Location quality ranking (Q_loc): precision in the location with respect to the trace of the Host Fault: A = precise location from available GPS and/or available tabulated data sets, or original field map (expected error in the order of a few meters to some tenths of m); B = approximate location from clear maps and

- sketch (expected error in the order of some hundreds of meters); C = approximate location from not fully clear maps and sketch (expected error up to 1 km).
- 21) Data resolution quality ranking (Q_res): precision in reporting the FSP attitude data (slickenside and slick-online) from the original reference source to the database: A = data from tablets and published tabulated dataset or original field booklets; B = FSP attitudes derived from clear published stereoplots projections (expected reproduction error in the order of 1–2°); C = FSP attitudes derived either from not so clear and easily readable published stereoplots projections or from fixed –90° rake for dip-slip faults (expected error up to about 5°).
 - 22) Reference (Ref): source paper used for deriving the SS location (Lat and Lon) and the FSP attitude (strike, dip, dip-angle, trend, and plunge). All remaining data from this database are calculated in this work. Data reference key: Alo13³⁰; Ama18⁶²; Bel21²⁸; Bel22³⁵; Bon22⁶³; B&S00⁶⁴; Bro09⁶⁵; Bro11⁶⁶; Bro17⁶⁷; Bru16⁶⁸; Cas02b⁶⁹; Cif04⁷⁰; Cif07⁷¹; DB05⁷²; DB06⁷³; DG13⁷⁴; Fac11⁷⁵; Fer08⁷⁶; Fer19⁷⁷; Fes03⁷⁸; FW12²⁶; Gam21⁷⁹; Ghi79⁸⁰; Imp10⁸¹; Jac01³⁶; Mac14⁸²; Mas05⁸³; San16⁸⁴; Scu20¹⁷; Sga20⁸⁵; Tan05⁸⁶; Tan07⁸⁷; Tan15⁸⁸; Tor95⁸⁹; Tri18⁹⁰. Data from this paper are labeled as “PP” (*i.e.*, present paper).
 - 23) Trend of the P₄₅-axis (P₄₅_trend; in degrees): trend of the shortening axis.
 - 24) Plunge of the P₄₅-axis (P₄₅_plunge; in degrees): plunge of the shortening axis.
 - 25) Trend of the B₄₅-axis (B₄₅_trend; in degrees): trend of the neutral axis.
 - 26) Plunge of the B₄₅-axis (B₄₅_plunge; in degrees): plunge of the neutral axis.
 - 27) Trend of the T₄₅-axis (T₄₅_trend; in degrees): trend of the extension axis.
 - 28) Plunge of the T₄₅-axis (T₄₅_plunge; in degrees): plunge of the extension axis.
 - 29) Trend of the P₃₀-axis (P₃₀_trend; in degrees): trend of the minimum extension axis.
 - 30) Plunge of the P₃₀-axis (P₃₀_plunge; in degrees): plunge of the minimum extension axis.
 - 31) Trend of the B₃₀-axis (B₃₀_trend; in degrees): trend of the neutral axis.
 - 32) Plunge of the B₃₀-axis (B₃₀_plunge; in degrees): plunge of the neutral axis.
 - 33) Trend of the T₃₀-axis (T₃₀_trend; in degrees): trend of the maximum extension axis.
 - 34) Plunge of the T₃₀-axis (T₃₀_plunge; in degrees): plunge of the maximum extension axis.

Host Faults database records description.

- 1) Ordinal Number (Ord_No): it uniquely identifies each fault trace (numbers increase from north to south).
- 2) Fault longitude start point (X_start): longitude of the trace start point in decimal degrees (dd.mmmmm; WGS84 reference frame).
- 3) Fault latitude start point (Y_start): latitude of the trace start point in decimal degrees (dd.mmmmm; WGS84 reference frame).
- 4) Fault longitude endpoint (X_end): longitude of the trace endpoint in decimal degrees (dd.mmmmm; WGS84 reference frame).
- 5) Fault latitude endpoint (Y_end): latitude of the trace endpoint in decimal degrees (dd.mmmmm; WGS84 reference frame).
- 6) Region (Reg): administrative region where the fault is located (in the case of multiple regions, they are all reported from north to south).
- 7) Host Fault Name (H_F): name of the fault hosting the SS.
- 8) Host Fault Key (HF_key): gives information on the generic dip-direction of the fault toward the Tyrrhenian Hinterland (east- to north-dipping normal faults in Fig. 1) or the Adriatic-Ionian Foreland (west- to south-dipping normal faults in Fig. 1).
- 9) Fault System Name (F_S): name of the fault system consisting of a number of along-strike or perpendicular-to-strike interconnected HF; “N_A” is reported for those HFs not included in a fault system.
- 10) Fault System Onset (F_S_Onset): the age of the oldest recorded displacement and/or of the oldest syn-tectonic deposits among the HFs attributed to the FS; “N_A” is reported for those HFs not included in a fault system.
- 11) Fault System Seismogenic Activity (F_S_Seism): evidence of seismogenic or potentially seismogenic activity from integrated geological and seismological data; “NaN” = no information.

Technical Validation

Of the 4,297 FSPs contained in the QUIN 2.0 release, 47% derive from new observations, while 53% are from the literature (Fig. 4a). The latter are subdivided into literature A (25%) and literature B (28%), which are internal (*i.e.*, at least one author of the present paper is author of the paper from that reference) and external (*i.e.*, no authors from this paper are authors of the literature B papers), respectively. As a whole, the new FSPs (47% of the database) and those from the internal literature (28%) represent more than 70% of the database information, giving a general guarantee of homogeneity in the survey methodology and database classification.

Following Lavecchia *et al.*¹, we assign two different quality rankings defined as Q_loc and Q_res, which represent the resolution of the source information in terms of localization and reproducibility of the FSP, respectively (Fig. 4a). Each quality ranking is subdivided into three classes from A to C, where A represent the most reliable. Regarding Q_loc, ~19% of the QUIN 2.0 FSP data falls into class A, ~78% into class B, and ~3% into class C (A is best). As for Q_Res, ~56% of the data are class A, ~43% class B, and ~1% class C (Fig. 4a).

Still, there are sources of uncertainty in constructing the QUIN databases. These can derive from the original accuracy in the field survey (*e.g.*, precision in measuring strikes and dips, trends and plunges), or from

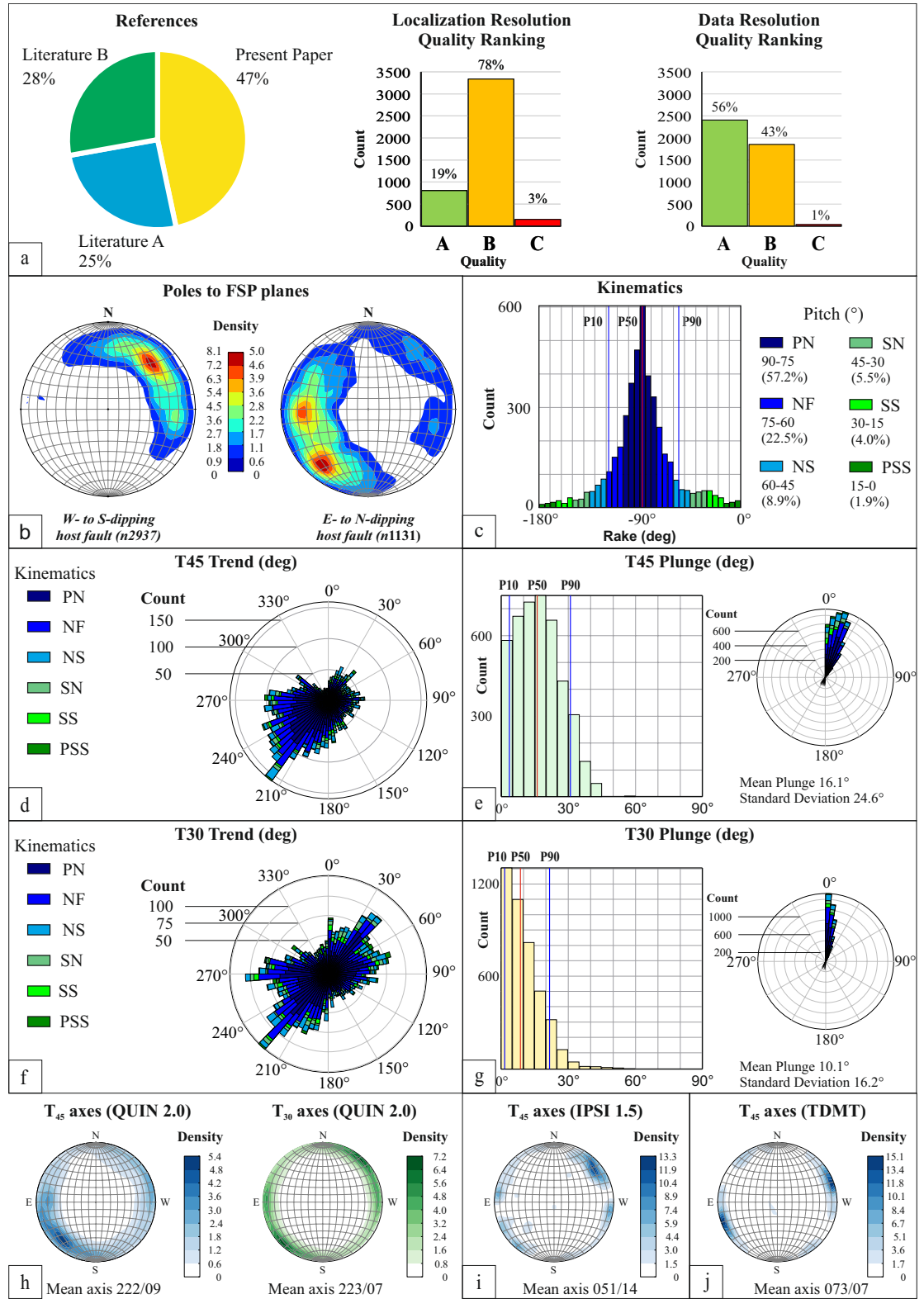


Fig. 4 Characteristics of the QUIN 2.0 database. **(a)** Cake diagram describing the percentage of FSP data original or derived from the literature (Literature A = references containing at least one of the authors of the present paper; B = other authors only). The histograms represent the quality rankings for FSP data localization and resolution (A is best). **(b)** Density contours of pole stereographic projections (poles to planes) subdivided for SS lying on Tyrrhenian and foreland-dipping Host Faults. The poles represented in the stereonet have been grouped on the basis of the Host Faults. To a Host Fault are associated major and minor fault planes falling within its damage zone, and which can therefore have synthetic or antithetic dip-direction with respect to the Host Fault (specified in the “Position” record in the database). **(c)** Rake histogram with rake-based kinematic bins and corresponding pitch angles with relative frequency expressed in percent (key: PN = Pure Normal fault, NF = Normal Fault, NS = Normal Strike-slip fault,

SN = Strike-slip Normal fault, SS = Strike-Slip fault, PSS = Pure Strike-Slip fault). (d) Trend rose diagram and plunge histogram (e) of the tensional deformation axis T_{45} , calculated assuming the fracture angle $\theta = 45^\circ$. (f) Trend rose diagram and plunge histogram (g) of the tensional deformation axis T_{30} , calculated assuming the fracture angle $\theta = 30^\circ$. (h) T-axis (T_{30} and T_{45}) density contours from this database, compared with the (i) T-axis density contours of the upper crust (depth < 15 km) focal mechanisms in the IPSI's database and with the (j) TDMT database, within the boundaries of the QUIN 2.0 study area.

imprecisions introduced by digitizing data from pre-existing maps and stereographic projections (*i.e.*, operator errors). In the first case, the data acquired with tablet computers or devices equipped with a gyroscope, magnetometer, accelerometer and integrated GPS are the most reliable, especially when checked by acquiring double measurements with a compass. In the second case, the uncertainty may be minimized by considering the quality parameter assigned to the source data (*i.e.*, Q_{res}) and making use of the Andrenacci *et al.*⁵⁵ tool, which highlights, by returning a warning, when the slickenline does not lie exactly on the fault plane.

Approximately 72% of the data is located on HFs dipping toward the Tyrrhenian-hinterland (or on associated antithetic minor structures; west- to south-dipping HF in Figs. 1, 4b), while ~28% is located on HFs dipping toward the Adriatic-Ionian foreland (or on associated antithetic minor structures; east- to north-dipping HF in Figs. 1, 4b). Predominant dip-slip kinematics is evident from the histogram (5° bin) of rake angle values in Fig. 4c. As also observed in the first release, a small percentage of data (~10%) shows a major strike-slip component, with tensional axes coaxial with extensional deformation on average. Figure 4d–g display the orientations (trend and plunge) of the FSP tensional axes (*i.e.*, T_{45} and T_{30}) here computed and highlight a near-optimal orientation for most of the FSPs if assuming the Andersonian conditions calculated with $\theta = 30^\circ$ (see also Lavecchia *et al.*¹). Further validation on the FSP comes from comparing these deformation axes with those of the contemporary stress field from focal mechanisms of the IPSI database⁷, and the TDMT¹²⁶. The comparison shows a substantial co-axiality of the Quaternary and present-day deformation field (Figs. 2, 4i,j).

Usage Notes

Uses of the QUIN database and supporting Host Faults shapefile are fully described in Lavecchia *et al.*¹. We here recall/highlight some main opportunities:

1. To provide geology-based deformation data and constraints on potentially seismogenic faults in peninsular Italy that lack seismological data due to inactivity in instrumental or historical times, making input data available for seismic hazard assessment.
2. To better identify and characterize seismogenic sources and the stress regime controlling their activity, through comparison of the long-term geological data with present-day geodetic^{49,127} and seismological information^{48,110}.
3. To guide geoscientists in the field for detailed studies on active tectonics, seismic hazard, structural geology and historical seismology^{18,19,21,31,38,85,128}.
4. To make available a large local-scale dataset that constrains the Quaternary deformation at a regional scale (*i.e.*, the whole Apennines), which can be particularly useful in complex areas (for example, the Calabrian Apennines close to the Benioff plane located offshore the Calabrian arc) or in areas known to be seismic gaps such as the Morrone fault system in the Abruzzo region¹²⁹ or the Pollino-Crati fault system in Lucania-Calabria^{19,67}.

These objectives may be achieved by exploiting QUIN data with different methods and approaches, including rake-angle interpolation, pseudo-focal mechanism computation^{28,51}, stress inversion^{19,130}, static-stress interaction analysis^{131,132}, and slip-tendency evaluation¹³³.

In conclusion, QUIN 1.0 and QUIN 2.0 databases together cover almost the entire extent of peninsular Italy for a length of more than 1,000 km along strike and an area of more than 32,000 km², making available an incredible amount of data (a total of 7,636 FSPs on 1,183 SSs) for future integrations and interpretations by the geological and geophysical scientific community.

Code availability

The MATLAB code we used in this work to obtain the FSP deformation axes was developed by Andrenacci *et al.*⁵⁵ for use in Lavecchia *et al.*¹ and is available from the ZENODO repository (<https://zenodo.org/record/5910783>)⁵⁵, together with a complete guide to use.

Received: 9 October 2023; Accepted: 22 January 2024;

Published online: 12 February 2024

References

1. Lavecchia, G. *et al.* QUaternary fault strain INDicators database - QUIN 1.0 - first release from the Apennines of central Italy. *Sci. Data* **9**, 204 (2022).
2. Barchi, M. R. The Neogene-Quaternary evolution of the Northern Apennines: crustal structure, style of deformation and seismicity. *J. Virtual Explor.* **36** (2010).
3. Papanikolaou, I. D. & Roberts, G. P. Geometry, kinematics and deformation rates along the active normal fault system in the southern Apennines: Implications for fault growth. *J. Struct. Geol.* **29**, 166–188 (2007).
4. Roberts, G. P. & Michetti, A. M. Spatial and temporal variations in growth rates along active normal fault systems: An example from The Lazio-Abruzzo Apennines, central Italy. *J. Struct. Geol.* **26**, 339–376 (2004).

5. Cohen, K. M., Finney, S. C., Gibbard, P. L. & Fan, J. X. The ICS International Chronostratigraphic Chart. *Episodes* **36**, 199–204 (2023).
6. Heidbach, O. *et al.* The World Stress Map database release 2016: Crustal stress pattern across scales. *Tectonophysics* **744**, 484–498 (2018).
7. Mariucci, M. T. & Montone, P. Database of Italian present-day stress indicators, IPSI 1.4. *Sci. Data* **7**, 298 (2020).
8. Mariucci, M. T. & Montone, P. Contemporary stress field in the area of the 2016 amatrice seismic sequence (Central Italy). *Ann. Geophys.* **59**, 1–9 (2016).
9. Montone, P. & Mariucci, M. T. The new release of the Italian contemporary stress map. *Geophys. J. Int.* **205**, 1525–1531 (2016).
10. Montone, P. & Mariucci, M. T. Deep well new data in the area of the 2022 Mw 5.5 earthquake, Adriatic Sea, Italy: In situ stress state and P-velocities. *Front. Earth Sci.* **11**, 1164929 (2023).
11. Bird, P., Ben-Avraham, Z., Schubert, G., Andreoli, M. & Viola, G. Patterns of stress and strain rate in southern Africa. *J. Geophys. Res.* **111**, B08402 (2006).
12. Delvaux, D. & Barth, A. African stress pattern from formal inversion of focal mechanism data. *Tectonophysics* **482**, 105–128 (2010).
13. Bello, S. *et al.* High-resolution surface faulting from the 1983 Idaho Lost River Fault Mw 6.9 earthquake and previous events. *Sci. Data* **8**, 68 (2021).
14. Maldonado, V., Contreras, M. & Melnick, D. A comprehensive database of active and potentially-active continental faults in Chile at 1:25,000 scale. *Sci. Data* **8**, 1–13 (2021).
15. Atanackov, J. *et al.* Database of Active Faults in Slovenia: Compiling a New Active Fault Database at the Junction Between the Alps, the Dinarides and the Pannonian Basin Tectonic Domains. *Front. Earth Sci.* **9** (2021).
16. Williams, J. N. *et al.* The Malawi Active Fault Database: An Onshore-Offshore Database for Regional Assessment of Seismic Hazard and Tectonic Evolution. *Geochem. Geophys. Geosyst.* **23**, e2022GC010425 (2022).
17. Scudero, S., De Guidi, G., Caputo, R. & Perdicaro, V. A semi-quantitative method to combine tectonic stress indicators: example from the Southern Calabrian Arc (Italy). *Bulletin of the Geological Society of Greece* **56**(1), 280–316 (2020).
18. De Guidi, G., Caputo, R. & Scudero, S. Regional and local stress field orientation inferred from quantitative analyses of extension joints: Case study from southern Italy. *Tectonics* **32**, 239–251 (2013).
19. Cirillo, D. *et al.* Structural complexities and tectonic barriers controlling recent seismic activity in the Pollino area (Calabria–Lucania, southern Italy) – constraints from stress inversion and 3D fault model building. *Solid Earth* **13**, 205–228 (2022).
20. Brutto, F. *et al.* In: *Moment Tensor Solutions*. (ed. D'Amico, S.) (Springer Natural Hazards, 2018).
21. Ferrarini, F., Lavecchia, G., de Nardis, R. & Brozzetti, F. Fault Geometry and Active Stress from Earthquakes and Field Geology Data Analysis: The Colfiorito 1997 and L'Aquila 2009 Cases (Central Italy). *PAGEOPH* **172**, 1079–1103 (2015).
22. Faure Walker, J. *et al.* Fault2SHA Central Apennines database and structuring active fault data for seismic hazard assessment. *Sci. Data* **8**, 1–20 (2021).
23. Villani, F. *et al.* Surface ruptures database related to the 26 December 2018, MW 4.9 Mt. Etna earthquake, southern Italy. *Sci. Data* **7**, 1–9 (2020).
24. Villani, F. *et al.* A database of the coseismic effects following the 30 October 2016 Norcia earthquake in Central Italy. *Sci. Data* **5** (2018).
25. Faure Walker, J. P. *et al.* Horizontal strain-rates and throw-rates across breached relay zones, central Italy: Implications for the preservation of throw deficits at points of normal fault linkage. *J. Struct. Geol.* **31**, 1145–1160 (2009).
26. Faure Walker, J. P. *et al.* Relationship between topography, rates of extension and mantle dynamics in the actively-extending Italian Apennines. *Earth Planet. Sci. Lett.* **325–326**, 76–84 (2012).
27. Guidoboni, E. *et al.* CFT15Med, the new release of the catalogue of strong earthquakes in Italy and in the Mediterranean area. *Sci. Data* **6**, 80 (2019).
28. Bello, S. *et al.* Fault Pattern and Seismotectonic Style of the Campania – Lucania 1980 Earthquake (Mw 6.9, Southern Italy): New Multidisciplinary Constraints. *Front. Earth Sci.* **8**, 608063 (2021).
29. Barreca, G. *et al.* The Strait of Messina: Seismotectonics and the source of the 1908 earthquake. *Earth Sci Rev* **218** (2021).
30. Aloisi, M. *et al.* Are the source models of the M 7.1 1908 Messina Straits earthquake reliable? Insights from a novel inversion and a sensitivity analysis of levelling data. *Geophys. J. Int.* **192**, 1025–1041 (2013).
31. Andrenacci, C. *et al.* Reappraisal and Analysis of Macroseismic Data for Seismotectonic Purposes: The Strong Earthquakes of Southern Calabria, Italy. *Geosciences* **13** (2023).
32. Burrato, P. & Valensise, G. Rise and fall of a hypothesized seismic gap: Source complexity in the Mw 7.0 16 December 1857 Southern Italy earthquake. *BSSA* **98**, 139–148 (2008).
33. Cello, G., Tondi, E., Micarelli, L. & Mattioni, L. Active tectonics and earthquake sources in the epicentral area of the 1857 Basilicata earthquake (southern Italy). *J. Geodyn.* **36**, 37–50 (2003).
34. Bello, S. *et al.* Coupling rare earth element analyses and high-resolution topography along fault scarps to investigate past earthquakes: A case study from the Southern Apennines (Italy). *Geosphere* **19**, 1348–1371 (2023).
35. Bello, S. *et al.* Complex trans-ridge normal faults controlling large earthquakes. *Sci. Rep.* **12**, 10676 (2022).
36. Jacques, E., Monaco, C., Taponnier, P., Tortorici, L. & Winter, T. Faulting and earthquake triggering during the 1783 Calabria seismic sequence. *Geophys. J. Int.* **147**, 499–516 (2001).
37. Pirrotta, C., Parrino, N., Pepe, F., Tansi, C. & Monaco, C. Geomorphological and Morphometric Analyses of the Catanzaro Trough (Central Calabrian Arc, Southern Italy): Seismotectonic Implications. *Geosciences* **12** (2022).
38. Galli, P. & Bosi, V. Catastrophic 1638 earthquakes in Calabria (southern Italy): New insights from paleoseismological investigation. *JGR Solid Earth* **108**, 1–20 (2003).
39. Galli, P. Nearly Simultaneous Pairs and Triplets of Historical Destructive Earthquakes with Distant Epicenters in the Italian Apennines. *Seismol. Res. Lett.* (2023).
40. de Nardis, R. *et al.* Lithospheric double shear zone unveiled by microseismicity in a region of slow deformation. *Sci. Rep.* **12**, 21066 (2022).
41. Brozzetti, F. *et al.* High-Resolution Field Mapping and Analysis of the August–October 2016 Coseismic Surface Faulting (Central Italy Earthquakes): Slip Distribution, Parameterization, and Comparison With Global Earthquakes. *Tectonics* **38**, 417–439 (2019).
42. Lavecchia, G., de Nardis, R., Cirillo, D., Brozzetti, F. & Boncio, P. The May–June 2012 Ferrara Arc earthquakes (northern Italy): Structural control of the spatial evolution of the seismic sequence and of the surface pattern of coseismic fractures. *Ann. Geophys.* **55**, 533–540 (2012).
43. Lavecchia, G. *et al.* From surface geology to aftershock analysis: Constraints on the geometry of the L'Aquila 2009 seismogenic fault system. *Ital. J. Geosci.* **131**, 330–347 (2012).
44. Mildon, Z. K., Roberts, G. P., Faure Walker, J. P., Wedmore, L. N. J. & McCaffrey, K. J. W. Active normal faulting during the 1997 seismic sequence in Colfiorito, Umbria: Did slip propagate to the surface? *J. Struct. Geol.* **91**, 102–113 (2016).
45. Panara, Y., Menegoni, N., Carboni, F. & Inama, R. 3D digital outcrop model-based analysis of fracture network along the seismogenic Mt. Vettore Fault System (Central Italy): the importance of inherited fractures. *J. Struct. Geol.* **161**, <https://doi.org/10.1016/j.jsg.2022.104654> (2022).
46. Civico, R. *et al.* Surface ruptures following the 30 October 2016 Mw6.5 Norcia earthquake, central Italy. *J. Maps* (2018).

47. Lavecchia, G. *et al.* Slowly Deforming Megathrusts within the Continental Lithosphere: A Case from Italy. *GSA Today* **34**, 4–10 (2023).
48. Rovida, A. *et al.* Catalogo Parametrico dei Terremoti Italiani (CPTI15), version 4.0. *Istituto Nazionale di Geofisica e Vulcanologia (INGV)* <https://doi.org/10.13127/CPTI/CPTI15.4> (2022).
49. Ferranti, L. *et al.* Rates of geodetic deformation across active faults in southern Italy. *Tectonophysics* **621**, 101–122 (2014).
50. Pizzi, A., Di Domenico, A., Gallovič, F., Luzi, L. & Puglia, R. Fault Segmentation as Constraint to the Occurrence of the Main Shocks of the 2016 Central Italy Seismic Sequence. *Tectonics* **36**, 2370–2387 (2017).
51. Bello, S. *et al.* High-Detail Fault Segmentation: Deep Insight into the Anatomy of the 1983 Borah Peak Earthquake Rupture Zone (Mw 6.9, Idaho, USA). *Lithosphere* **8100224** (2022).
52. Palo, M., Picozzi, M., De Landro, G. & Zollo, A. Microseismicity clustering and mechanic properties reveal fault segmentation in southern Italy. *Tectonophysics* **856** (2023).
53. Carboni, F. *et al.* Surface ruptures and off-fault deformation of the October 2016 central Italy earthquakes from DInSAR data. *Sci. Rep.* **12**, 3172 (2022).
54. Aki, K. & Richards, P. *Quantitative Seismology*. 2nd edn, (University Science Books U.S., 2002).
55. Andrenacci, C., Bello, S., de Nardis, R. & Lavecchia, G. Fault-Striation Pair analysis (F-SPA) Tool. *Zenodo* <https://doi.org/10.5281/zenodo.5910783> (2021).
56. Lavecchia, G. *et al.* Host Faults Database of central Italy [Data set]. *Zenodo* <https://doi.org/10.5281/zenodo.5603004> (2021).
57. Lavecchia, G., Bello, S., Cirillo, D., Pietrolungo, F. & Brozzetti, F. Quaternary-Host Faults Database 2.0 (Southern Italy). *Zenodo* <https://doi.org/10.5281/zenodo.10370819> (2023).
58. Lavecchia, G. The Tyrrhenian-Apennines system: structural setting and seismotectogenesis. *Tectonophysics* **147**, 263–296 (1988).
59. Vezzani, L., Festa, A. & Ghisetti, F. C. Geology and Tectonic Evolution of the Central-Southern Apennines, Italy. *The Geological Society of America Special Papers* **469**, 1–58 (2010).
60. Lavecchia, G. *et al.* Regional seismotectonic zonation of hydrocarbon fields in active thrust belts: a case study from Italy in *Building Knowledge for Geohazard Assessment and Management in the Caucasus and other Orogenic Regions* (eds Bonali F. L., Mariotto F. P., & Tsereteli N.) Ch. 7, 89–128 (Springer Netherlands, 2021).
61. Cultrera, F. *et al.* Active faulting and continental slope instability in the Gulf of Patti (Tyrrhenian side of NE Sicily, Italy): a field, marine and seismological joint analysis. *Natural Hazards* **86**, 253–272 (2016).
62. Amato, V. *et al.* Geomorphic response to late Quaternary tectonics in the axial portion of the Southern Apennines (Italy): A case study from the Calore River valley. *Earth Surf. Process. Landf.* **43**, 2463–2480 (2018).
63. Boncio, P. *et al.* Late Quaternary faulting in the southern Matese (Italy): implications for earthquake potential and slip rate variability in the southern Apennines. *Solid Earth* **13**, 553–582 (2022).
64. Bonini, M. & Sani, F. Pliocene-Quaternary transpressional evolution of the Anzi-Calvello and Northern S. Arcangelo basins (Basilicata, Southern Apennines, Italy) as a consequence of deep-seated fault reactivation. *Mar. Pet. Geol.* **17**, 909–927 (2000).
65. Brozzetti, F., Lavecchia, G., Mancini, G., Milana, G. & Cardinali, M. Analysis of the 9 September 1998 Mw 5.6 Mercure earthquake sequence (Southern Apennines, Italy): A multidisciplinary approach. *Tectonophysics* **476**, 210–225 (2009).
66. Brozzetti, F. The Campania-Lucania Extensional Fault System, southern Italy: A suggestion for a uniform model of active extension in the Italian Apennines. *Tectonics* **30**, 1–26 (2011).
67. Brozzetti, F. *et al.* Newly identified active faults in the Pollino seismic gap, southern Italy, and their seismotectonic significance. *J. Struct. Geol.* **94**, 13–31 (2017).
68. Brutto, F. *et al.* The Neogene-Quaternary geodynamic evolution of the central Calabrian Arc: A case study from the western Catanzaro Trough basin. *J. Geodyn.* **102**, 95–114 (2016).
69. Casciello, E., Pappone, G. & Zuppetta, A. Structural features of a shear-zone developed in an argillaceous medium: the southern portion of the Scoriabuoi fault (Southern Apennines). *Boll. soc. Geol. It.* **1**, 659–667 (2002).
70. Cifelli, F. *et al.* An AMS, structural and paleomagnetic study of quaternary deformation in eastern Sicily. *J. Struct. Geol.* **26**, 29–46 (2004).
71. Cifelli, F., Rossetti, F. & Mattei, M. The architecture of brittle postorogenic extension: Results from an integrated structural and paleomagnetic study in north Calabria (southern Italy). *Geol. Soc. Am. Bull.* **119**, 221–239 (2007).
72. Di Bucci, D., Naso, G., Corrado, S. & Villa, I. M. Growth, interaction and seismogenic potential of coupled active normal faults (Isernia Basin, central-southern Italy). *Terra Nova* **17**, 44–55 (2005).
73. Di Bucci, D., Massa, B. & Zuppetta, A. Relay ramps in active normal fault zones: A clue to the identification of seismogenic sources (1688 Sannio earthquake, Italy). *Geol. Soc. Am. Bull.* **118**, 430–448 (2006).
74. De Guidi, G. *et al.* Multidisciplinary study of the Tindari Fault (Sicily, Italy) separating ongoing contractional and extensional compartments along the active Africa–Eurasia convergent boundary. *Tectonophysics* **588**, 1–17 (2013).
75. Faccenna, C. *et al.* Topography of the Calabria subduction zone (southern Italy): Clues for the origin of Mt. Etna. *Tectonics* **30** (2011).
76. Ferranti, L., Monaco, C., Morelli, D., Antonioli, F. & Maschio, L. Holocene activity of the Scilla Fault, Southern Calabria: Insights from coastal morphological and structural investigations. *Tectonophysics* **453**, 74–93 (2008).
77. Ferranti, L. *et al.* Speleoseismological constraints on ground shaking threshold and seismogenic sources in the pollino range (Calabria, southern Italy). *JGR Solid Earth* **124**, 5192–5216 (2019).
78. Festa, V. Cretaceous structural features of the Murge area (Apulian Foreland, Southern Italy). *Eclogae Geol. Helv.* **96**, 11–22 (2003).
79. Gambino, S. *et al.* Deformation Pattern of the Northern Sector of the Malta Escarpment (Offshore SE Sicily, Italy): Fault Dimension, Slip Prediction, and Seismotectonic Implications. *Front. Earth Sci.* **8** (2021).
80. Ghisetti, F. Evoluzione neotettonica dei principali sistemi di faglie della Calabria centrale. *Boll. soc. Geol. It.* **98**, 387–430 (1979).
81. Improta, L. *et al.* Detecting young, slow-slipping active faults by geologic and multidisciplinary high-resolution geophysical investigations: A case study from the Apennine seismic belt, Italy. *JGR Solid Earth* **115**, 1–26 (2010).
82. Macri, P., Speranza, F. & Capraro, L. Magnetic fabric of Plio-Pleistocene sediments from the Crotona fore-arc basin: Insights on the recent tectonic evolution of the Calabrian Arc (Italy). *J. Geodyn.* **81**, 67–79 (2014).
83. Maschio, L., Ferranti, L. & Burrato, P. Active extension in Val d'Agri area, southern Apennines, Italy: Implications for the geometry of the seismogenic belt. *Geophys. J. Int.* **162**, 591–609 (2005).
84. Santaloia, F. *et al.* Coastal thermal springs in a foreland setting: The Santa Cesarea Terme system (Italy). *Geothermics* **64**, 344–361 (2016).
85. Sgambato, C., Faure Walker, J. P. & Roberts, G. P. Uncertainty in strain-rate from field measurements of the geometry, rates and kinematics of active normal faults: Implications for seismic hazard assessment. *J. Struct. Geol.* **131**, 103934 (2020).
86. Tansi, C., Iovine, G. & Gallo, M. F. Tettonica attiva e recente, e manifestazioni gravitative profonde, lungo il bordo orientale del graben del Fiume Crati (Calabria settentrionale). *boll. soc. Geol. It.* **124**, 563–578 (2005).
87. Tansi, C., Muto, F., Critelli, S. & Iovine, G. Neogene-Quaternary strike-slip tectonics in the central Calabrian Arc (southern Italy). *J. Geodyn.* **43**, 393–414 (2007).
88. Tansi, C. *et al.* in *GIS Day Calabria 2015*.
89. Tortorici, L., Monaco, C., Tansi, C. & Cocina, O. Recent and active tectonics in the Calabrian arc (Southern Italy). *Tectonophysics* **243**, 37–55 (1995).

90. Tripodi, V., Muto, F., Brutto, F., Perri, F. & Critelli, S. Neogene–Quaternary evolution of the forearc and backarc regions between the Serre and Aspromonte Massifs, Calabria (southern Italy). *Mar. Pet. Geol.* **95**, 328–343 (2018).
91. Galli, P. & Bosi, V. Paleoseismology along the Cittanova fault: Implications for seismotectonics and earthquake recurrence in Calabria (southern Italy). *J. Geophys. Res.* **107** (2002).
92. Galli, P., Bosi, V., Piscitelli, S., Giocoli, A. & Scionti, V. Late Holocene earthquakes in southern Apennine: Paleoseismology of the Caggiano fault. *Int. J. Earth Sci.* **95**, 855–870 (2006).
93. Spina, V., Tondi, E., Galli, P., Mazzoli, S. & Cello, G. Quaternary fault segmentation and interaction in the epicentral area of the 1561 earthquake (Mw = 6.4), Vallo di Diano, southern Apennines, Italy. *Tectonophysics* **453**, 233–245 (2008).
94. Galli, P. & Peronace, E. Low slip rates and multimillennial return times for Mw 7 earthquake faults in southern Calabria (Italy). *Geophys. Res. Lett.* **42**, 5258–5265 (2015).
95. Galli, P., Scionti, V. & Spina, V. New paleoseismic data from the Lakes and Serre faults; seismotectonic implications for Calabria (southern Italy). *Ital. J. Geosci.* **126**, 347–364 (2007).
96. Spina, V., Galli, P., Tondi, E., Critelli, S. & Cello, G. Kinematics and structural properties of an active fault zone in the Sila Massif (Northern Calabria, Italy). *Boll. soc. Geol. It.* **126**, 427–438 (2007).
97. Spina, V., Tondi, E., Galli, P. & Mazzoli, S. Fault propagation in a seismic gap area (northern Calabria, Italy): Implications for seismic hazard. *Tectonophysics* **476**, 357–369 (2009).
98. Amicucci, L., Barchi, M. R., Montone, P. & Rubiliani, N. The Vallo di Diano and Auletta extensional basins in the southern Apennines (Italy): A simple model for a complex setting. *Terra Nova* **20**, 475–482 (2008).
99. Cinti, F. R. *et al.* Integrating multidisciplinary, multiscale geological and geophysical data to image the Castrovillari fault (Northern Calabria, Italy). *Geophys. J. Int.* **203**, 1847–1863 (2015).
100. Cinti, F. R., Moro, M., Pantosti, D., Cucci, L. & D’Addezio, G. New constraints on the seismic history of the Castrovillari fault in the Pollino gap (Calabria, southern Italy). *J. Seismol.* **6**, 199–217 (2002).
101. Civile, D., Martino, C. & Zecchin, M. Contractual deformation and Neogene tectonic evolution of the Pergola–Melandro valley area (Southern Apennines). *GeoActa* **9**, 1–19 (2010).
102. Ferrarini, F. *et al.* Segmentation pattern and structural complexities in seismogenic extensional settings: The North Matese Fault System (Central Italy). *J. Struct. Geol.* **95**, 93–112 (2017).
103. Galli, P. & Scionti, V. Two unknown M>6 historical earthquakes revealed by palaeoseismological and archival researches in eastern Calabria (southern Italy). Seismotectonic implications. *Terra Nova* **18**, 44–49 (2006).
104. Molin, P., Fubelli, G. & Dramis, F. Evidence of tectonic influence on drainage evolution in an uplifting area: the case of the Northern Sila (Calabria, Italy). *Geogr. Fis. Dinam. Quat.* **35**, 46–90 (2012).
105. Giano, S. I. & Martino, C. Assetto morfotettonico e morfostratigrafico di alcuni depositi continentali pleistocenici del bacino del Pergola–Melandro (Appennino Lucano). *Italian Journal of Quaternary Sciences* **16**, 289–297 (2003).
106. Moro, M. *et al.* Surface evidence of active tectonics along the Pergola–Melandro fault: A critical issue for the seismogenic potential of the southern Apennines, Italy. *J. Geodyn.* **44**, 19–32 (2007).
107. Brozzetti, F. *et al.* Structural style of Quaternary extension in the Crati Valley (Calabrian Arc): Evidence in support of an east-dipping detachment fault. *Ital. J. Geosci.* **136**, 434–453 (2017).
108. Ascione, A., Cinque, A., Improta, L. & Villani, F. Late Quaternary faulting within the Southern Apennines seismic belt: new data from Mt. Marzano area (Southern Italy). *Quat. Int.* **101–102**, 27–41 (2003).
109. Dorsey, R. J., Longhitano, S. G. & Chiarella, D. Structure and morphology of an active conjugate relay zone, Messina Strait, southern Italy. *Basin Res.* **00**, 1–21 (2023).
110. Latorre, D., Di Stefano, R., Castello, B., Michele, M. & Chiaraluce, L. An updated view of the Italian seismicity from probabilistic location in 3D velocity models: The 1981–2018 Italian catalog of absolute earthquake locations (CLASS). *Tectonophysics* **846** (2023).
111. Civile, D., Schiattarella, M., Martino, C. & Zecchin, M. Geology of the Pergola–Melandro basin area, Southern Apennines, Italy. *J. Maps* **13**, 7–18 (2017).
112. Patacca, E. & Scandone, P. Geology of the Southern Apennines. *Bollettino della Società Geologica Italiana, Supplemento* **7**, 75–119 (2007).
113. Monaco, C., Tortorici, L., Nicolich, R., Cernobori, L. & Costa, M. From collisional to rifted basins: an example from the southern Calabrian arc (Italy). *Tectonophysics* **266**, 233–249 (1996).
114. Filice, F. *et al.* Geology map of the central area of Catena Costiera: insights into the tectono–metamorphic evolution of the Alpine belt in Northern Calabria. *J. Maps* **11**, 114–125 (2015).
115. Ghisetti, F. & Vezzani, L. Different styles of deformation in the calabrian arc (Southern Italy): Implications for a seismotectonic zoning. *Tectonophysics* **85**, 149–165 (1982).
116. Ercoli, M., Carboni, F., Akimbekova, A., Carbonell, R. B. & Barchi, M. R. Evidencing subtle faults in deep seismic reflection profiles: Data pre-conditioning and seismic attribute analysis of the legacy CROP-04 profile. *Front. Earth Sci.* **11** (2023).
117. Malinverno, A. & Ryan, W. B. F. Extension in the Tyrrhenian Sea and shortening in the Apennines as result of arc migration driven by sinking of the lithosphere. *Tectonics* **5**, 227–245 (1986).
118. D’Argenio, B., letto, A. & Oldow, J. S. Low angle normal faults in the Picentini Mountains (southern Italy). *Rend. Soc. Geol. It.* **9**, 113–125 (1987).
119. Ferranti, L. & Oldow, J. S. History and tectonic implications of low-angle detachment faults and orogen parallel extension, Picentini Mountains, Southern Apennines fold and thrust belt, Italy. *Tectonics* **18**, 498–526 (1999).
120. Casciello, E., Cesarano, M. & Pappone, G. Extensional detachment faulting on the Tyrrhenian margin of the southern Apennines contractional belt (Italy). *J. Geol. Soc.* **163**, 617–629 (2006).
121. Brozzetti, F., Boncio, P., Lavecchia, G. & Pace, B. Present activity and seismogenic potential of a low-angle normal fault system (Città di Castello, Italy): Constraints from surface geology, seismic reflection data and seismicity. *Tectonophysics* **463**, 31–46 (2009).
122. Cello, G. *et al.* Fault zone characteristics and scaling properties of the Val d’Agri Fault system (southern Apennines, Italy). *J. Geodyn.* **29**, 293–307 (2000).
123. Schiattarella, M. in *Continental Transpressional and Transtensional Tectonics* Vol. 135 (eds R. E. Holdsworth, R. A. Strachan, & J. F. Dewey) 341–354 (Geological Society, 1998).
124. Monaco, C., Tortorici, L. & Paltrinieri, W. Structural evolution of the Lucanian Apennines, southern Italy. *J. Struct. Geol.* **20**, 617–638 (1998).
125. Lavecchia, G. *et al.* QUIN 2.0 - new release of the QUaternary fault strain INDicators database from the Southern Apennines of Italy. *Zenodo* <https://doi.org/10.5281/zenodo.8414734> (2023).
126. Scognamiglio, L., Tinti, E. & Quiliani, M. *Istituto Nazionale di Geofisica e Vulcanologia (INGV)* <https://doi.org/10.13127/TDMTdata.2018.49> (2006).
127. De Guidi, G. *et al.* Brief communication: Co-seismic displacement on 26 and 30 October 2016 (Mw D 5.9 and 6.5) – earthquakes in central Italy from the analysis of a local GNSS network. *NHESS* **17**, 1885–1892 (2017).
128. Falcone, F. *et al.* Geo-archaeology, archaeometry, and history of a seismic-endangered historical site in central Apennines (Italy). *Herit Sci* **11**, 68 (2023).
129. Romano, M. A. *et al.* Temporary seismic monitoring of the Sulmona area (Abruzzo, Italy): a quality study of microearthquake locations. *NHESS* **13**, 2727–2744 (2013).

130. Sperner, B. *et al.* Tectonic stress in the Earth's crust: advances in the World Stress Map project. *J. Geol. Soc. London* **212**, 101–116 (2003).
131. Troise, C., De Natale, G., Pingue, F. & Petrazzuoli, S. M. Evidence for static stress interaction among earthquakes in the south-central Apennines (Italy). *Geophys. J. Int.* **134**, 809–817 (1998).
132. Giuffrida, S. *et al.* Multidisciplinary analysis of 3D seismotectonic modelling: a case study of Serre and Cittanova faults in the southern Calabrian Arc (Italy). *Frontiers in Earth Science* **11**, 1240051 (2023).
133. Morris, A., Ferrill, D. A. & Henderson, D. B. Slip-tendency analysis and fault reactivation. *Geology* **24**, 275–278 (1996).

Acknowledgements

This research was partially developed and supported by PRIN 2017 (2017KT2MKE) funds from the Italian Ministry of Education, University and Research granted to the P.I. Giusy Lavecchia. We also acknowledge all those who have helped, over the years, to develop the QUIN project with assistance and experience.

Author contributions

The first two authors, G.L. and S.B., contributed equally to the present paper to all stages of this research. G.L., S.B. and C.A. designed the QUIN database setting, did statistical analysis, and prepared the figures. S.B. and C.A. prepared the QUIN database tables. G.L., S.B. and D.C. designed and prepared the Host Fault database. F.B., S.B. and C.M. coordinated two ad-hoc field campaigns to fill gaps of data, in which D.C., C.A., F.P., D.T., M.M., Fi.C., S.Ga., G.D.G., G.B., S.Gi., C.P. and Fr.C. participated. G.R., J.F.W., C.S., F.B., S.B., D.C., C.M., G.D.G., L.F. and L.V. provided tabulated published and unpublished fault/slip data. C.A. S.B. and D.C., handled the fault/slip data compilation from literature and GIS representation. R.d.N., F.F., P.G., G.T. and M.R.B. contributed to the general discussion and technical validation of data. G.R., F.B. and P.G. supervised the methodological aspects and contributed to the geological validation of Host Fault traces. All authors have read and agreed to this version of the manuscript.

Competing interests

The authors declare no competing interests.

Additional information

Correspondence and requests for materials should be addressed to S.B.

Reprints and permissions information is available at www.nature.com/reprints.

Publisher's note Springer Nature remains neutral with regard to jurisdictional claims in published maps and institutional affiliations.



Open Access This article is licensed under a Creative Commons Attribution 4.0 International License, which permits use, sharing, adaptation, distribution and reproduction in any medium or format, as long as you give appropriate credit to the original author(s) and the source, provide a link to the Creative Commons licence, and indicate if changes were made. The images or other third party material in this article are included in the article's Creative Commons licence, unless indicated otherwise in a credit line to the material. If material is not included in the article's Creative Commons licence and your intended use is not permitted by statutory regulation or exceeds the permitted use, you will need to obtain permission directly from the copyright holder. To view a copy of this licence, visit <http://creativecommons.org/licenses/by/4.0/>.

© The Author(s) 2024